Clinical Neurophysiology 130 (2019) 2088–2095

Contents lists available at ScienceDirect

Clinical Neurophysiology

journal homepage: www.elsevier.com/locate/clinph

Relative contributions of diabetes and chronic kidney disease to neuropathy development in diabetic nephropathy patients

Tushar Issar [a], Ria Arnold [b], Natalie C.G. Kwai [a,c], Susan Walker [a], Aimy Yan [a], Adeniyi A. Borire [a], Ann M. Poynten [d], Bruce A. Pussell [e], Zoltan H. Endre [e], Matthew C. Kiernan [f], Arun V. Krishnan [a,*]

[a] Prince of Wales Clinical School, UNSW Sydney, NSW 2031, Australia
[b] School of Medical Sciences, UNSW Sydney, NSW 2052, Australia
[c] Department of Exercise Physiology, UNSW Sydney, NSW 2052, Australia
[d] Department of Endocrinology, Prince of Wales Hospital, Sydney, NSW 2031, Australia
[e] Department of Nephrology, Prince of Wales Hospital, Sydney, NSW 2031, Australia
[f] Brain and Mind Centre, University of Sydney and Royal Prince Alfred Hospital, Sydney, NSW 2050, Australia

ARTICLE INFO

Article history:
Accepted 12 August 2019
Available online 22 August 2019

Keywords:
Diabetic neuropathy
Diabetic kidney disease
Diabetic nephropathy
Chronic kidney disease
Uremic neuropathy
Nerve excitability

HIGHLIGHTS

- Patients with DKD manifest a more severe neuropathy phenotype and greater nerve dysfunction.
- The pathophysiological mechanisms between DKD and CKD are similar.
- These findings suggest that CKD and not T2DM propels axonal dysfunction in DKD.

ABSTRACT

Objective: Chronic kidney disease (CKD) caused by diabetes is known as diabetic kidney disease (DKD). The present study aimed to examine the underlying mechanisms of axonal dysfunction and features of neuropathy in DKD compared to CKD and type 2 diabetes (T2DM) alone.
Methods: Patients with DKD ($n = 30$), CKD ($n = 28$) or T2DM ($n = 40$) and healthy controls ($n = 41$) underwent nerve excitability assessments to examine axonal function. Neuropathy was assessed using the Total Neuropathy Score. A validated mathematical model of human axons was utilised to provide an indication of the underlying causes of nerve pathophysiology.
Results: Total neuropathy score was significantly higher in patients with DKD compared to those with either CKD or T2DM ($p < 0.05$). In DKD, nerve excitability measures (S2 accommodation and superexcitability, $p < 0.05$) were more severely affected compared to both CKD and T2DM and worsened with increasing serum K^+ ($p < 0.01$). Mathematical modelling indicated the basis for nerve dysfunction in DKD was an elevation of extracellular K^+ and reductions in Na^+ permeability and the hyperpolarisation-activated cation current, which was similar to CKD.
Conclusions: Patients with DKD manifested a more severe neuropathy phenotype and shared features of nerve dysfunction to that of CKD.
Significance: The CKD, and not diabetes component, appears to underlie axonal pathophysiology in DKD.

1. Introduction

Diabetic kidney disease (DKD) is the chronic loss of renal function due to diabetes. The leading cause of chronic kidney disease (CKD) is type 2 diabetes (T2DM) and the growing incidence of T2DM has led to an increase in DKD worldwide (Tuttle et al., 2014). Peripheral neuropathy is one of the most common complications of both T2DM and CKD (Aggarwal et al., 2013; Feldman et al., 2017). The most frequent clinical manifestation of peripheral

Abbreviations: CKD, chronic kidney disease; DKD, diabetic kidney disease; I_h, hyperpolarisation-activated cation current; T2DM, type 2 diabetes; TNS, total neuropathy score.

* Corresponding author at: Institute of Neurological Sciences, Prince of Wales Hospital, Randwick, NSW 2031, Australia.
E-mail address: arun.krishnan@unsw.edu.au (A.V. Krishnan).

https://doi.org/10.1016/j.clinph.2019.08.005
1388-2457/

neuropathy in both conditions is a distal symmetric polyneuropathy, which is characterised by initial sensory loss and impaired reflexes in the lower limbs with subsequent muscle weakness and atrophy (Krishnan and Kiernan, 2009; Pop-Busui et al., 2017). Peripheral neuropathy in diabetes is known as diabetic neuropathy and affects at least 50% of patients (Feldman et al., 2017). In CKD, peripheral neuropathy affects approximately 70% of predialysis patients (Hanewinckel et al., 2017). The overlap of diabetes and CKD is thought to contribute to a more rapid onset of nerve injury in patients who have both conditions, however the relative effects of each condition in DKD has not been explored (Pop-Busui et al., 2010).

The aim of the study was to assess the difference in neuropathy phenotype in DKD compared to T2DM and CKD alone and evaluate the relative contributions of T2DM and CKD to nerve dysfunction in DKD. Peripheral nerve pathophysiology in each condition was assessed using nerve excitability techniques, which provide an insight into the activity of ion channels, pumps, and exchangers of the axonal membrane. For each cohort, nerve excitability values were evaluated in a mathematical model of the human motor nerve to provide precise data on the exact location of the pathological change in the peripheral nerves of each disease group.

2. Methods

2.1. Subjects

This study was approved by the South East Sydney Area Health Service Human Research Ethics Committee (Northern Section) and the Human Research Ethics Committee of the University of New South Wales. All subjects enrolled provided written informed consent to the procedures in accordance with the Declaration of Helsinki. A total of 98 patients with T2DM, CKD, or DKD were consecutively recruited from the Diabetes Mellitus Centre and Kidney Care Centre at the Prince of Wales Hospital in Sydney, Australia. Required sample size was calculated based on nerve excitability measures that have previously been demonstrated to be abnormal in in T2DM and CKD (superexcitability and S2 accommodation) with 80% power (Arnold et al., 2017; Kwai et al., 2013). Allocation into the T2DM group was predicated on a clinical diagnosis of T2DM for at least one year and an estimated glomerular filtration rate (eGFR) greater than 80 mL/min/1.73 m^2. Inclusion into the CKD group was based on a clinical diagnosis of stage 3 or 4 CKD (eGFR between 15–59 ml/min/1.73 m^2) (National Kidney Foundation, 2002) and an absence of T2DM. Assignment into the DKD group required both a clinical diagnosis of T2DM and stage 3 or 4 CKD. Patients were excluded from participating in the study if they had any of the following: renal transplant, neurotoxic/neuromodulatory treatment, carpal tunnel syndrome, peripheral oedema, an additional condition known to cause neuropathy, or a neuromuscular, movement, psychiatric, or developmental disorder. 41 healthy controls were recruited for comparison.

Patient demographic, serum biochemistry, and clinical data of interest included age, sex, glycated haemoglobin A_{1c} (HbA_{1c}), eGFR, body mass index (BMI), serum K^+, urea, creatinine, and neuropathy severity, which was evaluated using the Total Neuropathy Score (TNS). The TNS is a validated instrument to evaluate peripheral neuropathy in diabetes, CKD, and DKD (Cornblath et al., 1999; Issar et al., 2018). The TNS is comprised of eight domains that assess sensory and motor peripheral nerve function and each domain is scored from 0 to 4. These eight domains are: sensory and motor symptoms, vibration (128 Hz tuning fork) and pinprick sensation (Neurotip™, Owen Mumford, United Kingdom), deep tendon reflexes, manual muscle strength, and sural sensory nerve (SNAP) and tibial motor nerve amplitude (CMAP) (Medelec Synergy, Oxford Instruments, UK). Total neuropathy scores range from 0 to 32 and a higher score is indicative of more severe neuropathy while a score of zero indicates an absence of neuropathy.

2.2. Nerve excitability studies

Nerve excitability was assessed at the median nerve using the TROND protocol as applied by Qtrac software (Digitimer, London, United Kingdom). The median nerve was orthodromically stimulated through surface electrodes (Ambu, Sydney, Australia), proximal to the wrist at the site of least resistance using a DS5 Isolated Bipolar Current Stimulator (Digitimer, London, United Kingdom). Compound muscle action potentials (CMAP) were recorded from the abductor pollicis brevis muscle. Skin temperature at the point of stimulation was kept above 32 °C (Burke et al., 1999; Kiernan et al., 2001). The excitability assessment consisted of four distinct testing paradigms which provide indirect information regarding the activity of voltage-gated sodium (Na^+) and potassium (K^+) ion channels, energy-dependent pumps, and exchangers embedded within the axon membrane at the point of stimulation. Stimulus-response curves were first generated using a 1 ms test pulse to obtain the maximal CMAP amplitude and a target response of 40% of maximum was calculated. The current required to elicit this target response, known as 'threshold', was tracked in the four excitability testing paradigms: strength–duration behaviour, threshold electrotonus, current–threshold relationship, and recovery cycle.

1. Strength–duration behaviour was examined by plotting the relationship between the stimulus intensity required to reach threshold from four different stimulus durations (0.2, 0.4, 0.8, and 1.0 ms). Weiss' Law was then applied to calculate the strength–duration time constant, which is a marker of persistent Na^+ conductance in the Node of Ranvier (Krarup and Moldovan, 2009).
2. Threshold electrotonus examines the changes in threshold in response to depolarising (stimulating) or hyperpolarising (inhibiting) conditioning currents. These changes were determined after a 1 ms test pulse is applied during or after 100 ms of a subthreshold conditioning current of + 40% (depolarising) or −40% (hyperpolarising) of control threshold, established from the initial stimulus-response curve. Percentage change in threshold was plotted at 10 ms intervals and key excitability measures (threshold change between 10 and 20 ms and S2 accommodation) were extracted from the plot. S2 accommodation is the specific phase of depolarising threshold electrotonus in which threshold reduction is limited and begins to return to control level. Threshold electrotonus assesses various nodal and internodal conductances, which contribute to the excitability of peripheral nerves and the ionic maintenance of their intracellular and extracellular environment (Bostock et al., 1998; Kiernan et al., 2000).
3. The current–threshold relationship quantifies rectification properties of the internode in response to long-lasting polarising currents (Bostock et al., 1998; Kiernan et al., 2000). This relationship was determined by plotting the percentage threshold change of 1 ms test pulses following 200 ms polarising currents ranging from +50% (depolarising) to −100% (hyperpolarising) of the control threshold. The minimum I-V slope represents the minimum slope calculated by fitting a straight line between three adjacent points.
4. The recovery cycle examines the changes in threshold following a nerve impulse. Percentage change in threshold was plotted for a range of conditioning–test intervals following a 1 ms supramaximal conditioning stimulus. The relative refractory period,

superexcitability, and subexcitability measures were subsequently determined. The recovery cycle assesses the activity of nodal Na^+ channels and fast K^+ ion channels (Bostock et al., 1998).

2.3. Mathematical modelling

To investigate the pathological basis for axonal dysfunction in each disease, nerve excitability recordings obtained from groups were further analysed using the Bostock model of axonal excitability, which is a validated model of the human axon based on a single node and internode connected by pathways through and under the myelin sheath (Bostock et al., 1991; Jankelowitz et al., 2007; Kiernan et al., 2005). The model assists in the interpretation of excitability findings between control and disease data by providing an indication of the underlying changes in and around the axonal membrane in the disease state. This includes changes in the maximal conductance and permeabilities of different types of Na^+ and K^+ ion channels, alterations in pump currents, biophysical properties, and surrounding ionic concentrations (Fig. 1). The model was first adjusted to fit the mean nerve excitability data obtained from the control group before fitting the mean data of the T2DM, CKD, or DKD group. Modelling of each disease was approached with a hypothesis based on factors previously implicated in nerve dysfunction. Transient and persistent Na^+ channels were modelled at the node whereas fast and slow K^+ channels were modelled in the node and internode. Currents through these Na^+ and K^+ channels were modelled as permeabilities, in accordance with the Constant-Field Theory (Boërio et al., 2014). Pump and leak currents and axolemmal capactiances were assessed in both compartments. The hyperpolarisation-activated cation current (I_h), which carries Na^+ and K^+ ions, was modelled only in the internode. Extracellular K^+ and the Barrett-Barrett conductance, which represents current flow between the node and internode through and underneath the myelin sheath, were also investigated (Howells et al., 2012). To better account for the effect of extracellular K^+, the permeabilities of fast and slow K^+ channels were made proportional to extracellular K^+ (Boërio et al., 2014). Modelling analyses involved changes in a single or a combination of parameters in an iterative fashion to objectively fit simulated excitability data with the mean recorded data as closely as possible using a least squares approach. The 'discrepancy' between the simulated and recorded data was obtained by the comparing the error between simulated and recorded data of the four excitability paradigms: strength-duration behaviour, threshold electrotonus, current-threshold relationship, and recovery cycle. Weighting factors of these paradigms were 0.5, 1, 1, and 2, respectively and were kept constant for the modelling of each disease. Minimum interstimulus interval for the recovery cycle was set at 3 ms. Analyses were run in unclamped mode to permit secondary changes in resting membrane potential caused by changes in conductances or pump currents.

2.4. Statistical analyses

Results were analysed using SPSS Statistics Version 25.0 for Windows (IBM Corp, New York, USA). Shapiro–Wilk tests were undertaken to determine the normality of data. Where appropriate and with post-hoc tests if required, a one-way analysis of variance, Kruskal-Wallis tests, independent t-tests, Mann–Whitney U tests, Pearson chi-square analyses were applied to compare means of demographic data, clinical measures and extracted nerve excitability variables between groups. Relationships between demographic and clinical data with nerve excitability variables were investigated using bivariate correlations in the form of a Pearson correlation coefficient (r) or a Spearman's rank correlation coefficient (ρ). Statistical significance was considered when $p < 0.05$.

3. Results

3.1. Subject demographics

Patient demographics were representative of the various disease cohorts (summarised in Table 1). The DKD group was matched for age and sex with T2DM and CKD groups. No difference was observed in diabetes duration, percentage of patients receiving insulin, glycaemic control and BMI between diabetes cohorts. Kidney filtration, urea, and creatinine were matched between DKD and CKD groups. All disease groups were matched for serum K^+. No significant differences were found in male to female ratio between disease cohorts and controls ($p = 0.194$).

3.2. Neuropathy scoring

Assessment of the total neuropathy scores and subscores for the eight items of the TNS established that patients with patients with DKD had a significantly higher total neuropathy score compared to patients with T2DM ($p = 0.019$) and CKD ($p = 0.020$; Table 2). Significantly higher subscores in DKD were observed in the TNS domains of motor nerve conduction amplitude (Tibial CMAP: vs. T2DM,

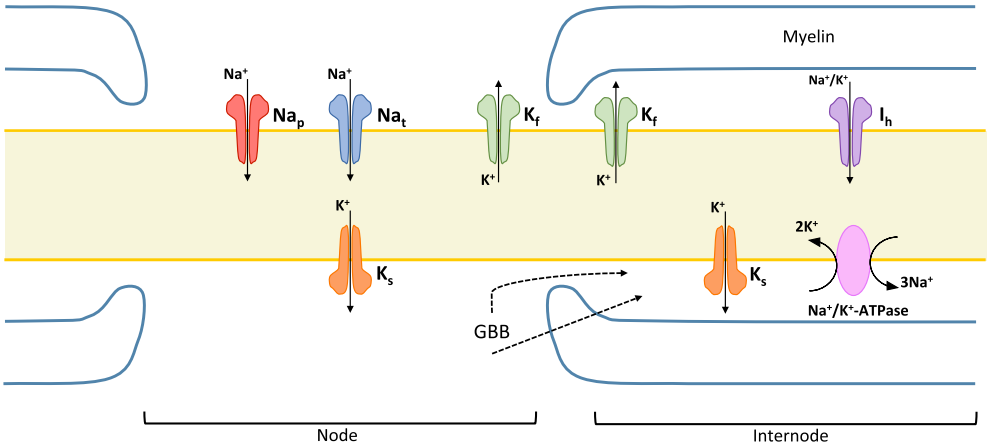

Fig. 1. Schematic of the peripheral nerve membrane highlighting the two compartments of the axon and the parameters that were modelled. Parameters investigated included: voltage-gated sodium (Na^+) channels (transient, Na_t and persistent, Na_p), voltage gated-potassium (K^+) ion channels (fast and slow), sodium-potassium pump (Na^+/K^+-ATPase), the hyperpolarisation-activated activated cation current (I_h) and the Barrett-Barrett conductance (GBB), which is the flow of current between the node and internode through and under the myelin sheath.

Table 1
Subject demographics.

	DKD (n = 30)	T2DM (n = 40)	CKD (n = 28)	Control (n = 41)	p value		
					DKD vs. T2DM	DKD vs. CKD	DKD vs. Control
Age (years)	66 (61–69)	59 ± 10	59 (50–71)	55 (54–59)	0.113	0.374	<0.001
Sex (% male)	50	51	63	73	–	–	–
BMI (kg/m^2)	32 (27–36)	30 ± 5	27 ± 5	25 (23–27)	0.203	0.004	<0.001
HbA_{1c} (%)	7.6 (7.3–8.9)	7.7 (6.8–9.4)	–	–	0.753	–	–
Diabetes duration (years)	15 ± 8	11 ± 7	–	–	0.126	–	–
Patients on Insulin (%)	67	65	–	–	–	–	–
eGFR (mL/min/1.73 m^2)	39 ± 10	90 (87–90)	33 ± 11	–	<0.001	0.097	–
K^+ (mmol/L)	4.6 ± 0.5	4.6 (4.4–4.9)	4.7 ± 0.4	–	0.826	0.581	–
Urea (mmol/L)	11.2 (9.3–15.6)	5.1 (3.5–6.0)	11.7 (9.8–13.1)	–	<0.001	0.539	–
Creatinine (mmol/L)	155 (125–187)	70 (62.1–80)	151 (137–178)	–	<0.001	0.522	–

Normally distributed data is expressed as mean ± SD while non-normally distributed data is expressed as median and quartile 1 to quartile 3.

p = 0.008; vs. CKD, p = 0.002) and sensory nerve conduction amplitude (Sural SNAP: vs. T2DM, p = 0.003; vs. CKD, p = 0.011). In DKD, the greatest impairment was seen in sensory nerve conduction while motor symptoms and manual muscle strength items had the lowest subscore values.

3.3. Nerve excitability

Nerve excitability findings are presented in Fig. 2 and extracted variables are summarised in Table 3. Patients with DKD exhibited severe abnormalities in excitability measures compared to patients with either T2DM or CKD. In DKD, there was a significant reduction in S2 accommodation (p = 0.007) and minimum I/V slope (p = 0.001) when compared to T2DM. Further, there was marked increase in superexcitability (p = 0.003) and decrease in subexcitability (p = 0.003) in the recovery cycle. Compared to patients with only CKD, patients with DKD demonstrated significant increases in superexcitability (p = 0.030) and the strength-duration time constant (p = 0.025) and a reduction in S2 accommodation (p = 0.025) Across all disease groups, no other differences in depolarising or hyperpolarising threshold electrotonus or in the current-threshold relationship were found. No correlation was found between total neuropathy score and excitability indices. Compared to controls, patients with DKD demonstrated significantly worse changes in all nerve excitability parameters, with the exception of the strength-duration time constant.

Nerve excitability measures in the CKD and T2DM cohorts were also found to be abnormal when compared to the control group (Table 3). Patients with CKD or T2DM exhibited decreases in S2 accommodation (CKD: p = 0.033; T2DM: p = 0.015) and subexcitability (CKD: p < 0.001; T2DM: p = 0.001) and increases in superexcitability (CKD: p = 0.019; T2DM: p = 0.003) and in the undershoot phase of depolarising threshold electrotonus (CKD: p = 0.011; T2DM: p = 0.005). Additionally, depolarising threshold electrotonus at 10–20 ms was reduced (p = 0.015 and the relatively refractory period was increased (p = 0.018) in CKD but not T2DM.

In DKD and CKD, increasing serum K^+ significantly correlated with more severe changes in nerve excitability variables. In DKD, increase in serum K^+ was associated with more severe alterations in various phases of depolarising threshold electrotonus (10–20 ms: r = −0.680, p < 0.001; S2 accommodation: r = −0.526, p = 0.003, undershoot: r = 0.423, p = 0.022) and recovery cycle (superexcitability: r = 0.660, p < 0.001; relative refractory period: ρ = 0.409, p = 0.034). In CKD, higher serum K^+ correlated with worsening depolarising threshold electrotonus at 10–20 ms (r = −0.390, p = 0.044) and superexcitability (r = 0.464, p = 0.017). In contrast, no relationship was found between serum K^+ and abnormal excitability measures in T2DM. In DKD and CKD, no association was found between urea or creatinine levels and nerve excitability variables. No relationship was observed between HbA_{1c} and excitability parameters in DKD and T2DM.

3.4. Mathematical modelling

Nerve excitability findings were modelled by varying membrane properties previously implicated in nerve dysfunction in each condition and findings are summarised in Fig. 3 and Table 4. Analysis of the DKD findings indicated that alterations in nerve excitability recordings were due to an elevation of extracellular K^+ concentration (Control: 3.6; DKD: 4.4, mmol/L) and a 20% reduction in Na^+ permeability (Control: 4.8; DKD: 3.85, $cm^3\ s^{-1} \times 10^{-9}$). A considerable improvement in the model could be achieved by a 26% reduction in I_h conductance (Control: 5.5; DKD: 4.05, nanosiemens). Together, these alterations in the model reduced the discrepancy between the Control group and patients with DKD by 86%.

Modelling of the CKD data was similar to the DKD data, particularly in relation to Na^+ permeability and I_h conductance.

Table 2
Total neuropathy score and subscore comparison.

	DKD (n = 30)	T2DM (n = 40)	CKD (n = 28)	Control (n = 41)	p value	
					DKD vs. T2DM	DKD vs. CKD
Total neuropathy score	9.2 ± 1.4	5.3 ± 1.0	4.9 ± 1.1	0	0.019	0.020
Sensory symptoms	1.0 ± 0.2	1.0 ± 0.2	0.9 ± 0.2	0	0.691	0.513
Motor symptoms	0.4 ± 0.2	0.3 ± 0.1	0.4 ± 0.1	0	0.286	0.811
Pinprick sensation	0.9 ± 0.2	0.5 ± 0.1	0.8 ± 0.2	0	0.108	0.678
Vibration sensation	1.4 ± 0.3	0.8 ± 0.2	0.8 ± 0.2	0	0.070	0.086
Strength	0.4 ± 0.2	0.3 ± 0.1	0.1 ± 0.1	0	0.353	0.103
Tendon reflexes	1.6 ± 0.3	1.3 ± 0.2	0.9 ± 0.2	0	0.302	0.043
Tibial CMAP	1.3 ± 0.3	0.4 ± 0.2	0.2 ± 0.2	0	0.008	0.002
Sural SNAP	2.0 ± 0.3	0.8 ± 0.2	0.8 ± 0.2	0	0.003	0.011

All data is expressed as mean ± SEM. CMAP: compound muscle action potential; SNAP: sensory nerve action potential.

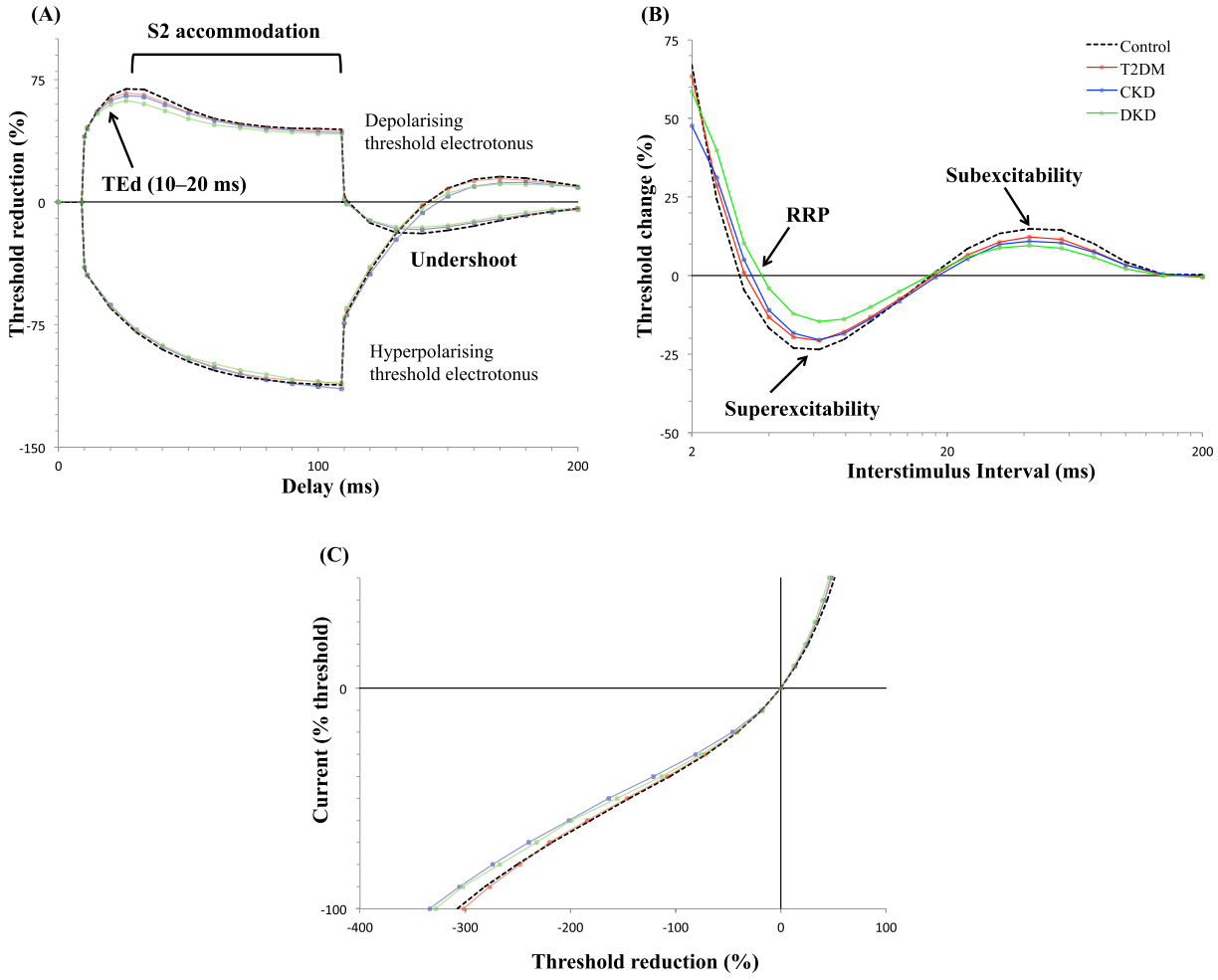

Fig. 2. Mean excitability data for patients with T2DM, CKD or DKD and healthy controls for the threshold electrotonus (A), recovery cycle (B) and current-threshold paradigms (C).

Table 3
Nerve excitability findings.

	DKD (n = 30)	T2DM (n = 40)	CKD (n = 28)	Control (n = 41)	p value				
					DKD vs. T2DM	DKD vs. CKD	DKD vs. Control	CKD vs. Control	T2DM vs. Control
SDTC (ms)	0.46 ± 0.01	0.48 ± 0.02	0.41 ± 0.02	0.44 ± 0.01	0.499	0.025	0.368	0.197	0.052
TEd (10–20 ms) (%)	61.7 ± 1.4	65.4 ± 1.1	64.0 ± 1.1	67.9 ± 0.9	0.075	0.350	0.001	0.015	0.079
TEd (S2) (%)	18.7 ± 0.7	21.1 ± 0.5	21.0 ± 0.7	22.9 ± 0.5	0.007	0.025	<0.001	0.033	0.015
Minimum I/V slope	0.22 ± 0.01	0.26 ± 0.01	0.24 ± 0.01	0.26 ± 0.01	0.001	0.271	0.001	0.084	0.999
Superexcitability (%)	−15.4 ± 1.2	−19.9 ± 0.9	−19.7 ± 1.5	−23.6 ± 0.9	0.003	0.030	<0.001	0.019	0.003
Subexcitability (%)	9.4 ± 0.7	11.9 ± 0.5	11.0 ± 0.6	14.6 ± 0.6	0.003	0.080	<0.001	<0.001	0.001
RRP (ms)	3.7 ± 0.2	3.3 ± 0.1	3.5 ± 0.1	3.2 ± 0.1	0.091	0.545	0.006	0.018	0.125

By convention, all excitability data is expressed as mean ± SEM with the exception of strength-duration time constant, minimum I/V slope and RRP. SDTC: strength-duration time constant; TEd: depolarising threshold electrotonus; S2: S2 accommodation phase; I/V: current-threshold; RRP: relative refractory period.

It revealed the simplest explanation for nerve excitability changes was a combination of a 15% decrease in Na^+ permeability (Control: 4.8; CKD: 4.1, $cm^3\ s^{-1} \times 10^{-9}$) and a 28% reduction in I_h conductance (Control: 5.5; CKD: 3.95, nanosiemens). These variations could account for 85% of the discrepancy between the two groups, which was considerably more than any other two-parameter combination.

Mathematical modelling of the T2DM data was quite different to both DKD and CKD. It demonstrated that the changes in T2DM were best explained by altering a range of conductances and permeabilities through ion channels in the node and the internode, as previously demonstrated in studies of type 1 diabetes (Kwai et al., 2016). Specifically, the changes were best accounted for by a decrease in Na^+ permeability and slow nodal K^+ channel permeability as well as an increase in the percentage of persistent Na^+ channels and fast K^+ channel permeability. Together, these changes accounted for 79% of the discrepancy between the Control and T2DM groups.

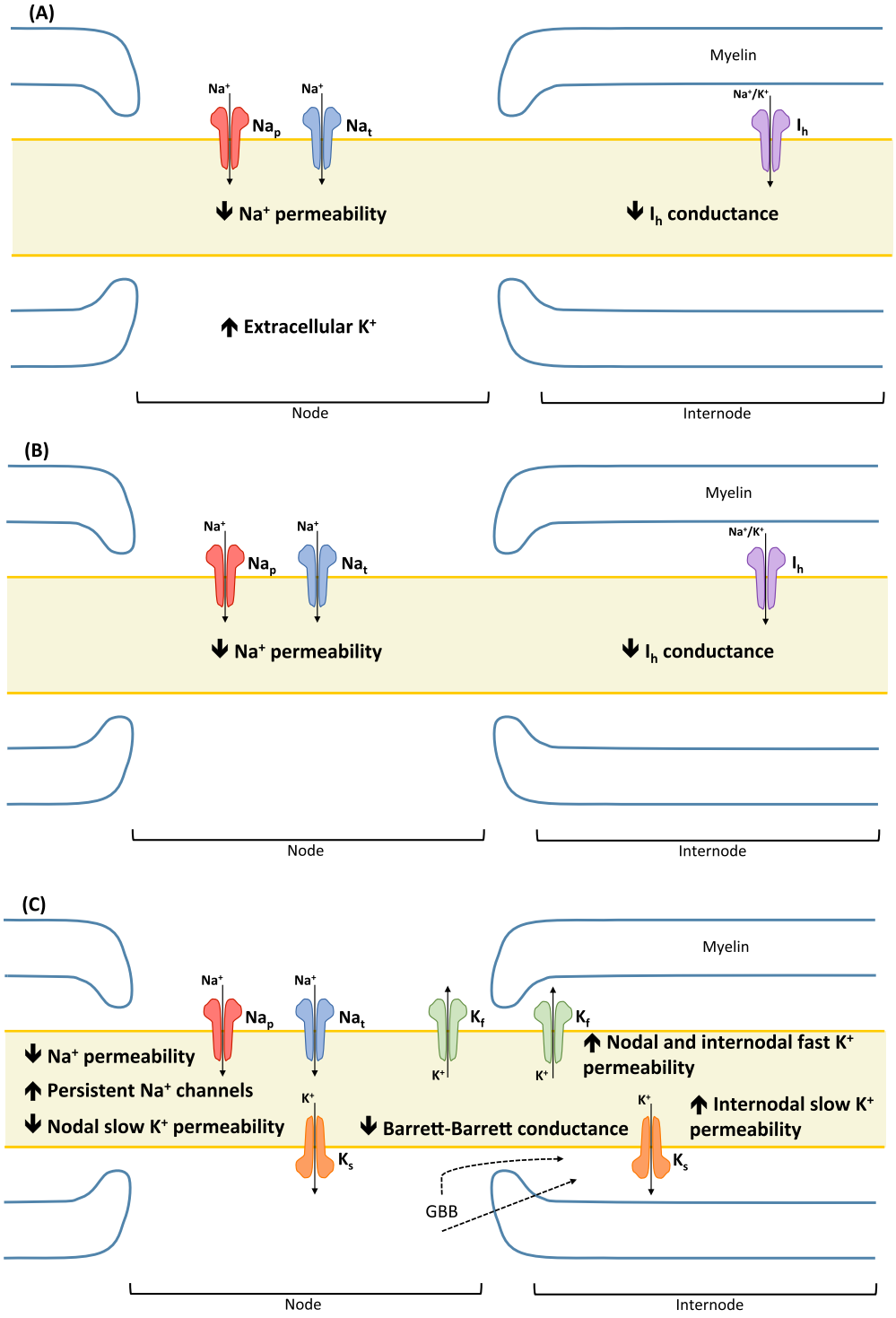

Fig. 3. Summary of mathematical modelling of nerve excitability data for diabetic kidney disease (A), chronic kidney disease (B), and type 2 diabetes (C). Pathophysiological mechanisms underlying nerve dysfunction in diabetic kidney disease are similar to those of chronic kidney disease.

4. Discussion

This study has provided evidence that DKD patients exhibit more severe neuropathy and greater nerve dysfunction when compared to patients with either CKD or T2DM alone. Patients with DKD had a higher total neuropathy score and exhibited greater reductions in motor and sensory nerve conduction amplitudes when compared to either T2DM or CKD alone, which suggests that the combined pathological effects of diabetic and uraemic neuropathy results in more severe nerve injury (Table 2). Consistent with these findings, patients with DKD demonstrated greater nerve dysfunction, as assessed by nerve excitability techniques, when compared to either T2DM or CKD (Table 3). Specifically, more severe alterations in S2 accommodation and superexcitability were observed in DKD. The magnitude of change was similar to previously reported measures in type 2 diabetes patients with severe diabetic neuropathy (total neuropathy scores ranging from 24 to 32) and patients with end-stage kidney disease

Table 4
Modelled parameters between DKD, CKD, T2DM, and control cohorts.

Parameter	DKD	CKD	T2DM	Control
Permeability of Na^+ channels at node ($cm^3\ s^{-1} \times 10^{-9}$)	3.85	4.1	4.05	4.8
% of Na^+ channels that are persistent (%)			0.835	0.69
Permeability of nodal slow K^+ channels ($cm^3\ s^{-1} \times 10^{-9}$)			0.48	0.56
Permeability of internodal slow K^+ channels ($cm^3\ s^{-1} \times 10^{-9}$)			0.0064	0.006
Permeability of nodal fast K^+ channels ($cm^3\ s^{-1} \times 10^{-9}$)			0.25	0.2
Permeability of internodal fast K^+ channels ($cm^3\ s^{-1} \times 10^{-9}$)			1.53	1.35
Barrett-Barrett conductance (nS)			33	33.9
Hyperpolarisation-activated cation current (nS)	4.05	3.95		5.5
Extracellular K^+ (mmol/L)	4.4			3.6

Key parameter changes applied in the mathematical model for disease cohorts from control values. Conductance values are expressed in nanosiemens (nS).

(Borire et al., 2017; Kwai et al., 2013). A significantly larger, and apparent normalisation of, the strength-duration time constant was present in DKD compared to CKD. It is hypothesised that this is due the increase of persistent Na^+ current that occurs in diabetic neuropathy (Kwai et al., 2013; Misawa et al., 2009). Significant differences in subexcitability and minimum I/V slope were also evident between DKD and T2DM but not CKD. Nerve dysfunction was also evident in CKD and T2DM alone when compared to healthy controls. While serum K^+ was within normal range in both DKD and CKD, increasing K^+ nevertheless correlated with greater abnormalities in nerve function. This was not the case in T2DM. Further, no correlation was found between HbA_{1c} and excitability measures in DKD and T2DM. Mathematical modelling suggested the underlying causes of peripheral nerve dysfunction in DKD mirrored those previously implicated in CKD, rather than T2DM.

Mathematical modelling of the DKD nerve excitability indicated that the underlying basis for nerve dysfunction was an elevation in extracellular K^+ to 4.4 mmol/L in conjunction with reductions in Na^+ permeability and the hyperpolarisation-activated cation current. The finding that axonal dysfunction was partially driven by an increase in K^+ from both the modelling and correlation analyses suggests that the CKD component has a greater role in nerve dysfunction in DKD. This is further supported by clinical trial data which have demonstrated that dietary potassium restriction, which is thought to reduce nerve injury due to CKD, appears to have an equally beneficial role in CKD patients with diabetes as CKD patients without diabetes (Arnold et al., 2017).

In the CKD cohort, abnormalities in nerve excitability were present even though the mean serum K^+ concentration of 4.7 mmol/L fell within normal range. Increasing K^+ correlated with greater nerve dysfunction, which is consistent with previous findings from a randomised controlled trial of dietary K^+ restriction in CKD in which it was demonstrated that the maintenance of serum K^+ - $\leq$ 4.5 mmol/L is neuroprotective (Arnold et al., 2017). The results of the current investigation suggest that peripheral nerves in CKD patients are especially susceptible to the development of abnormal excitability properties even within the high normal range for serum K^+. This argument is further supported by previous excitability studies in patients with end-stage renal failure without diabetes, in which an elevation of K^+ instead of other suspected uraemic toxins was implicated in axonal dysfunction (Arnold et al., 2014; Krishnan et al., 2005). Modelling analysis of the CKD data indicated that the changes in nerve excitability were due a decrease in the permeability of Na^+ at the node and conductance of I_h in the internodal compartment of the axon, which is underneath the myelin sheath. The decrease in Na^+ permeability is consistent with findings in experimental uraemic neuropathy (Brismar and Tegnèr, 1984). Alteration in I_h may be a reflection of structural changes in Schwann cells, such as swelling, that occurs with submyelinic accumulation of K^+ or the impaired buffering of internodal K^+ by these cells (Baker, 2002; Brazhe et al., 2011; Said, 2013).

Mathematical modelling of the excitability data in the T2DM cohort were consistent with previous studies of specific nodal and internodal ion channels in clinical and experimental T2DM (Table 4). The pattern of a decrease in Na^+ permeability and increase in the percentage of persistent Na^+ has been observed in human and animal studies (Brismar et al., 1987; Hong and Wiley, 2006; Krishnan and Kiernan, 2005; Misawa et al., 2009). Peripheral nerve biopsies from neuropathic T2DM patients and T2DM animal models have also demonstrated there is diffuse redistribution of fast K^+ channels from their juxtaparanodal position, which may explain the increase in permeability of these channels in both compartments of the axon (Zenker et al., 2012). The alterations in the nodal and internodal conductances and permeabilities determined from the modelling analysis of the T2DM excitability recordings are similar to findings in type 1 diabetes, with the exception of the Barrett-Barrett conductance (Kwai et al., 2016). In contrast to T2DM, it was observed that the Barrett-Barrett conductance (current flow between the node and internode through and underneath the myelin sheath) is increased in type 1 diabetes. It should however be noted there were differences in neuropathy severity between the diabetes groups of these two studies, as patients with type 1 diabetes in Kwai et al. (2016) were neuropathy-free and patients with T2DM in the present study had established neuropathy. Further, potassium channel function was modelled as a conductance in Kwai et al. (2016) as opposed to permeability, which has been shown to be more accurate (Boërio et al., 2014).

While we have provided evidence that CKD primarily underlies nerve pathophysiology in DKD, given that the DKD cohort exhibited more severe neuropathy than either the CKD or T2DM groups, the pathological effects of T2DM are likely to be involved in some way. Studies of insulin signalling in DKD have led to the proposal that insulin resistance is a key factor in the decline of renal function (Karalliedde and Gnudi, 2016). Greater insulin resistance is independently associated with the development of microalbuminuria and is thought to cause an escalation in oxidative stress and pro-inflammatory mediators in the kidney (Karalliedde and Gnudi, 2016; Parvanova et al., 2006). Consequently, this would initiate nerve injury via pathways implicated in uraemic neuropathy. Interestingly, insulin has also been shown to be a potent neurotrophic factor and insulin receptors are abundantly expressed on peripheral nerves (Feldman et al., 2017). The greater severity of neuropathy and nerve dysfunction observed in the DKD compared to T2DM may therefore be in part due to greater insulin resistance in DKD, which may result in an inability of peripheral nerves to respond to trophic support.

In conclusion, patients with DKD manifest a more severe neuropathy phenotype and greater nerve dysfunction than patients with either T2DM or CKD alone. Analysis of nerve excitability findings in DKD suggests the CKD component of the condition has a major role in causing axonal dysfunction. Future clinical studies of diabetic neuropathy should examine and report renal status of patients as a complicating pathophysiological factor.

Acknowledgements

The Total Neuropathy Score (TNS) was provided to Professor Arun Krishnan by Professor David Cornblath and Johns Hopkins University.

Declaration of Competing Interest

None.

Financial Support

RA was supported by an Early Career Post-Doctoral Fellowship of the National Health and Medical Research Council of Australia (#1091006). MCK was supported by a NHMRC Practitioner Fellowship (1156093); and by ForeFront, a large collaborative research group dedicated to the study of neurodegenerative diseases and funded by the National Health and Medical Research Council of Australia Program Grant (#1132524).

Authors' contributions

TI, RA, and AVK were involved in the research idea and study design. TI, RA, NCGK, SW, AY, and AAB acquired data. All authors were involved in data analysis and interpretation as well as revision of the manuscript.

References

Aggarwal HK, Sood S, Jain D, Kaverappa V, Yadav S. Evaluation of spectrum of peripheral neuropathy in predialysis patients with chronic kidney disease. Ren Fail 2013;35(10):1323–9. https://doi.org/10.3109/0886022X.2013.828261.

Arnold R, Pussell BA, Howells J, Grinius V, Kiernan MC, Lin CS, et al. Evidence for a causal relationship between hyperkalaemia and axonal dysfunction in end-stage kidney disease. Clin Neurophysiol 2014;125(1):179–85. https://doi.org/10.1016/j.clinph.2013.06.022.

Arnold R, Pianta TJ, Pussell BA, Kirby A, O'Brien K, Sullivan K, et al. Randomized, controlled trial of the effect of dietary potassium restriction on nerve function in CKD. Clin J Am Soc Nephrol 2017;12(10):1569–77. https://doi.org/10.2215/cjn.00670117.

Baker MD. Electrophysiology of mammalian Schwann cells. Prog Biophys Mol Biol 2002;78(2):83–103. https://doi.org/10.1016/S0079-6107(02)00007-X.

Boërio D, Bostock H, Spescha R, Z'Graggen WJ. Potassium and the excitability properties of normal human motor axons in vivo. PLoS One 2014:;9(6):e98262.

Borire AA, Arnold R, Pussell BA, Kwai NC, Visser LH, Simon NG, et al. Effects of haemodialysis on intraneural blood flow in end-stage kidney disease. Muscle Nerve 2017. https://doi.org/10.1002/mus.25704.

Bostock H, Baker M, Reid G. Changes in excitability of human motor axons underlying post-ischaemic fasciculations: evidence for two stable states. J Physiol 1991;441(1):537–57. https://doi.org/10.1113/jphysiol.1991.sp018766.

Bostock H, Cikurel K, Burke D. Threshold tracking techniques in the study of human peripheral nerve. Muscle Nerve 1998;21(2):137–58. https://doi.org/10.1002/(SICI)1097-4598(199802)21:2%3C137::AID-MUS1%3E3.0.CO;2-C.

Brazhe AR, Maksimov GV, Mosekilde E, Sosnovtseva OV. Excitation block in a nerve fibre model owing to potassium-dependent changes in myelin resistance. Interface Focus 2011;1(1):86–100. https://www.doi.org/10.1098/rsfs.2010.0001.

Brismar T, Tegnèr R. Experimental uremic neuropathy: Part 2. Sodium permeability decrease and inactivation in potential clamped nerve fibers. J Neurol Sci 1984;65(1):37–45. https://doi.org/10.1016/0022-510X(84)90065-0.

Brismar T, Sima AA, Greene DA. Reversible and irreversible nodal dysfunction in diabetic neuropathy. Ann Neurol 1987;21(5):504–7. https://doi.org/10.1002/ana.410210515.

Burke D, Mogyoros I, Vagg R, Kiernan MC. Temperature dependence of excitability indices of human cutaneous afferents. Muscle Nerve 1999;22(1):51–60. https://www.doi.org/10.1002/(SICI)1097-4598(199901)22:13.0.CO;2-Q.

Cornblath DR, Chaudhry V, Carter K, Lee D, Seysedadr M, Miernicki M, et al. Total neuropathy score: validation and reliability study. Neurology 1999;53(8):1660–4. https://doi.org/10.1212/WNL.53.8.1660.

Feldman EL, Nave KA, Jensen TS, Bennett DL. New horizons in diabetic neuropathy: mechanisms, bioenergetics, and pain. Neuron 2017;93(6):1296–313. https://doi.org/10.1016/j.neuron.2017.02.005.

Hanewinckel R, Ikram MA, Franco OH, Hofman A, Drenthen J, van Doorn PA. High body mass and kidney dysfunction relate to worse nerve function, even in adults without neuropathy. J Peripher Nerv Syst 2017;22(2):112–20. https://doi.org/10.1111/jns.12211.

Hong S, Wiley JW. Altered expression and function of sodium channels in large DRG neurons and myelinated A-fibers in early diabetic neuropathy in the rat. Biochem Biophys Res Commun 2006;339(2):652–60. https://doi.org/10.1016/j.bbrc.2005.11.057.

Howells J, Trevillion L, Bostock H, Burke D. The voltage dependence of I(h) in human myelinated axons. J Physiol 2012;590(7):1625–40. https://www.doi.org/10.1113/jphysiol.2011.225573.

Issar T, Arnold R, Kwai NCG, Pussell BA, Endre ZH, Poynten AM, et al. The utility of the Total Neuropathy Score as an instrument to assess neuropathy severity in chronic kidney disease: a validation study. Clin Neurophysiol 2018;129(5):889–94. https://doi.org/10.1016/j.clinph.2018.02.120.

Jankelowitz SK, Howells J, Burke D. Plasticity of inwardly rectifying conductances following a corticospinal lesion in human subjects. J Physiol 2007;581(Pt 3):927–40. https://doi.org/10.1113/jphysiol.2006.123661.

Karalliedde J, Gnudi L. Diabetes mellitus, a complex and heterogeneous disease, and the role of insulin resistance as a determinant of diabetic kidney disease. Nephrol Dial Transplant 2016;31(2):206–13. https://www.doi.org/10.1093/ndt/gfu405.

Kiernan MC, Burke D, Andersen KV, Bostock H. Multiple measures of axonal excitability: a new approach in clinical testing. Muscle Nerve 2000;23(3):399–409. https://doi.org/10.1002/(SICI)1097-4598(200003)23:3%3C399::AID-MUS12%3E3.0.CO;2-G.

Kiernan MC, Cikurel K, Bostock H. Effects of temperature on the excitability properties of human motor axons. Brain 2001;124(Pt 4):816–25. https://doi.org/10.1093/brain/124.4.816.

Kiernan MC, Isbister GK, Lin CS, Burke D, Bostock H. Acute tetrodotoxin-induced neurotoxicity after ingestion of puffer fish. Ann Neurol 2005;57(3):339–48. https://www.doi.org/10.1002/ana.20395.

Krarup C, Moldovan M. Nerve conduction and excitability studies in peripheral nerve disorders. Curr Opin Neurol 2009;22(5):460–6. https://doi.org/10.1097/WCO.0b013e3283304c9d.

Krishnan AV, Phoon RK, Pussell BA, Charlesworth JA, Bostock H, Kiernan MC. Altered motor nerve excitability in end-stage kidney disease. Brain 2005;128(Pt 9):2164–74. https://www.doi.org/10.1093/brain/awh558.

Krishnan AV, Kiernan MC. Altered nerve excitability properties in established diabetic neuropathy. Brain 2005;128(Pt 5):1178–87. https://www.doi.org/10.1093/brain/awh476.

Krishnan AV, Kiernan MC. Neurological complications of chronic kidney disease. Nat Rev Neurol 2009;5(10):542–51. https://doi.org/10.1038/nrneurol.2009.138.

Kwai NC, Arnold R, Wickremaarachchi C, Lin CS, Poynten AM, Kiernan MC, et al. Effects of axonal ion channel dysfunction on quality of life in type 2 diabetes. Diabetes Care 2013;36(5):1272–7. https://doi.org/10.2337/dc12-1310.

Kwai NC, Arnold R, Poynten AM, Howells J, Kiernan MC, Lin CS, et al. In vivo evidence of reduced nodal and paranodal conductances in type 1 diabetes. Clin Neurophysiol 2016;127(2):1700–6. https://doi.org/10.1016/j.clinph.2015.11.047.

Misawa S, Sakurai K, Shibuya K, Isose S, Kanai K, Ogino J, et al. Neuropathic pain is associated with increased nodal persistent Na+ currents in human diabetic neuropathy. J Peripher Nerv Syst 2009;14(4):279–84. https://www.doi.org/10.1111/j.1529-8027.2009.00239.x.

National Kidney Foundation. K/DOQI clinical practice guidelines for chronic kidney disease: evaluation, classification, and stratification. Am J Kidney Dis 2002;39(2 Suppl 1):S1–266.

Parvanova AI, Trevisan R, Iliev IP, Dimitrov BD, Vedovato M, Tiengo A, et al. Insulin resistance and microalbuminuria: a cross-sectional, case-control study of 158 patients with type 2 diabetes and different degrees of urinary albumin excretion. Diabetes 2006;55(5):1456–62. https://doi.org/10.2337/db05-1484.

Pop-Busui R, Roberts L, Pennathur S, Kretzler M, Brosius FC, Feldman EL. The management of diabetic neuropathy in CKD. Am J Kidney Dis 2010;55(2):365–85. https://doi.org/10.1053/j.ajkd.2009.10.050.

Pop-Busui R, Boulton AJ, Feldman EL, Bril V, Freeman R, Malik RA, et al. Diabetic neuropathy: a position statement by the American diabetes association. Diabetes Care 2017;40(1):136–54. https://doi.org/10.2337/dc16-2042.

Said G. Uremic neuropathy. Handb Clin Neurol 2013;115:607–12. https://www.doi.org/10.1016/B978-0-444-52902-2.00035-7.

Tuttle KR, Bakris GL, Bilous RW, Chiang JL, de Boer IH, Goldstein-Fuchs J, et al. Diabetic kidney disease: a report from an ADA Consensus Conference. Am J Kidney Dis 2014;64(4):510–33. https://doi.org/10.1053/j.ajkd.2014.08.001.

Zenker J, Poirot O, de Preux Charles AS, Arnaud E, Medard JJ, Lacroix C, et al. Altered distribution of juxtaparanodal kv1.2 subunits mediates peripheral nerve hyperexcitability in type 2 diabetes mellitus. J Neurosci 2012;32(22):7493–8. https://doi.org/10.1523/jneurosci.0719-12.2012.